Transit Times in Ultra-Relativistic Heavy-Ion Collisions

G. Wolschin

Z. Naturforsch. **46a**, 1037–1042 (1991); received May 18, 1991

Mean transit times in heavy-ion collisions are calculated as functions of the relativistic incident energy and the impact parameter. As a consequence of special relativity, they become constant in a central collision of ^{16}O with Pb at $T \simeq 0.15$ TeV. Together with a geometrical estimate of the maximum energy densities in the interaction region, it is argued that heavy ions in a large hadron collider may produce a quark-gluon plasma due to the plateau in the transit times at ultra-relativistic energies.

Key words: Heavy-ion collisions; Ultra-relativistic energies; Transit times; Energy densities; Quark-gluon plasma.

1. Introduction

Nuclear interaction times in heavy-ion collisions determine whether nonequilibrium processes such as particle transfer at lower energies or – possibly – the formation of a quark-gluon plasma at relativistic energies [1] reach the corresponding equilibrium limits. Although contact times do not represent observable quantities, the concept [2] has proven to be successful [3] in the description of heavy-ion reactions at incident energies T which are small compared to the rest mass m_0 of the projectile. Phenomenological calculations of mean interaction times have been a valuable tool for investigating the evolution of observables such as the distribution of fragment mass, energy and angular momentum in diffusion models of deeply inelastic collisions. The comparison with experiment has generally been quite satisfactory, and also the justification of the models on the basis of microscopic theories has made advances.

These earlier calculations do not consider the effects of special relativity. Whereas this is certainly justified at low bombarding energies $T/m_0 < 0.1$, the relativistic effects are not negligible in the transition region ($\gamma \approx 2$) at Bevalac- or SIS-energies $T/m_0 \approx 1$, and they have be considered at high energies $T/m_0 > 10$, where $\gamma > 10$.

As a complement to elaborate microscopic calculations of the collision dynamics in this energy region [4], a straightforward macroscopic calculation of mean transit times as functions of incident energy and impact parameter is presented together with an estimate of the maximum energy density that could be obtained in the equilibrium limit. Analogously to macroscopic models at low energies, the microscopic structure of the nuclei is not considered at this stage; in a more refined model, the description of individual nucleon-nucleon-collisions, quark degrees of freedom and the corresponding time scales – in particular, the interaction times τ_{int} – will have to be considered. In Sect. 2 the calculation of the mean transit time τ is outlined. In Sect. 3 the available energy in the interaction region is calculated and the maximum energy density attainable in the equilibrium limit is estimated for three model systems as functions of laboratory energy. The conclusions are drawn in Section 4.

2. Mean Transit Times: A Geometrical Model

To calculate the dependence of the transit time of a Lorentz-contracted projectile nucleus such as ^{16}O through a target nucleus on the incident energy and impact parameter in the target restframe, I start from the relativistic expression for the kinetic energy ($c \equiv 1$)

$$T = m_0(\gamma - 1)\,. \tag{2.1}$$

The corresponding projectile velocity

$$v = (1-\gamma^{-2})^{1/2} = \left[1 - \left(1 + \frac{T}{m_0}\right)^{-2}\right]^{1/2} \tag{2.2}$$

can be expanded to yield $(2\,T/m_0)^{1/2}$ in the non-relativistic limit, as expexted. A projectile nucleus with

Reprint requests to Dr. G. Wolschin, Postfach 10 26 40, W-6900 Heidelberg 1.

0932-0784 / 91 / 1200-1037 $ 01.30/0. – Please order a reprint rather than making your own copy.

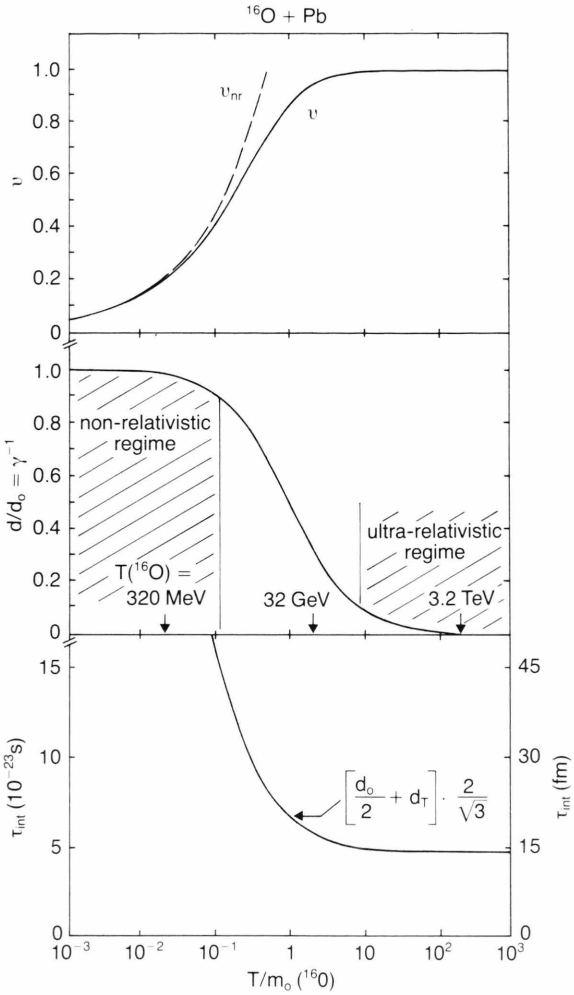

Fig. 1. Transit time τ for central collisions $^{16}O + Pb$ as a function of the laboratory energy T (lower curve). The plateau at large energies corresponds to the relativistic limit of the velocity v, upper curve; v_{nr} is the projectile velocity in the non-relativistic limit. The curve in the middle displays γ^{-1}.

diameter $d_0 = 2.4\,A^{1/3}$ fm is Lorentz-contracted in the direction of motion according to

$$d = d_0 \gamma^{-1} = d_0 \left(1 + \frac{T}{m_0}\right)^{-1}. \tag{2.3}$$

Hence, we have $\gamma = d_0/d \approx 2$ in the SIS-energy region $T \approx m_0$, whereas $d_0/d \simeq 216$ for 3.2 TeV ^{16}O-projectiles: the collision is safely within the ultra-relativistic region, Figure 1. The mean transit time of the center of the contracted projectile nucleus with diameter $d_0 \gamma^{-1}$ through the target nucleus with an extension $d_T(b)$ in the direction of motion at impact parameter b can then be calculated as

$$\tau(b) = [d_0 \gamma^{-1} + d_T(b)]\, v^{-1}$$
$$= [d_0 \gamma^{-1} + d_T(b)] \left[1 - \left(1 + \frac{T}{m_0}\right)^{-2}\right]^{-1/2}. \tag{2.4}$$

For a typical energy in the transition region $T/m_0 = 1$ ($\gamma = 2$) this becomes simply

$$\tau^{\gamma=2}(b) = \frac{2}{\sqrt{3}} \left[\frac{d_0}{2} + d_T(b)\right], \tag{2.5}$$

and in the ultra-relativistic limit $T/m_0 > 10$, $\tau^{\infty} = d_T(b)$ is obtained, as expected.

The energy dependence of the transit time for central collisions is displayed in Fig. 1: after a decrease of the time with increasing incident energy in the transition region, it rapidly levels off and reaches the ultra-relativistic plateau. The constancy of the mean transit time at high bombarding energies is of special interest since non-equilibrium processes such as energy deposition and plasma formation may easily reach the equilibrium limit. (Note that the time in the presence of interactions τ_{int} is necessarily larger than τ.) Hence, the situation is fundamentally different from collisions at lower energy where the interaction time decreases rapidly with increasing energy. Note, however, that the plateau value of the transit time

$$\tau^{\infty}(O + Pb) \simeq 4.6 \cdot 10^{-23}\,\text{s} \tag{2.6}$$

is two orders of magnitude smaller than typical interaction times [2] in low-energy heavy-ion collisions.

To obtain the mean transition time in the ultra-relativistic (plateau-)region as a function of impact parameter b, the transit distance $d_T(b)$ through the target nucleus with radius $R = r_0 A_T^{1/3}$ is calculated, and an average over the contracted projectile disk with radius $r = r_0 A_T^{1/3}$ is performed:

$$\tau(b) = \frac{1}{2r} \int_{b-r}^{b+r} 2 \cdot (R^2 - b'^2)^{1/2}\, db' \tag{2.7}$$
$$= \frac{1}{2r} \left\{(b+r)\,[R^2 - (b+r)^2]^{1/2} + R^2 \arcsin \frac{b+r}{R} + (r-b)\,[R^2 - (b-r)^2]^{1/2} - R^2 \arcsin \frac{b-r}{R}\right\}.$$

In the limit of central collisions, this yields

$$\tau(0) = [R^2 - r^2]^{1/2} + \frac{R^2}{r} \arcsin \frac{r}{R} \tag{2.8}$$

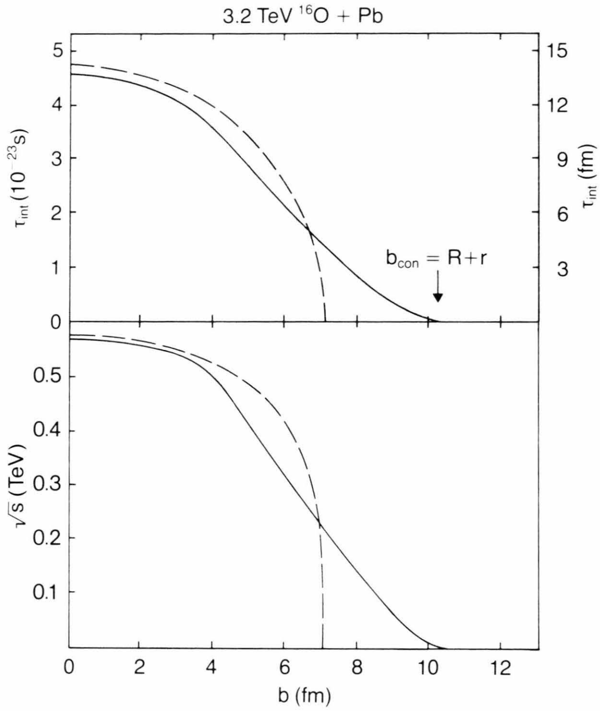

Fig. 2. Transit time τ for 3.2 TeV $^{16}O + Pb$ in the ultra-relativistic limit as function of impact parameter b (upper part). The target and projectile radii are denoted by R and r, respectively. In the result shown by the dashed curve, the finite extension of the projectile is neglected. In the lower part, the available center-of-mass energy is displayed as function of impact parameter.

with the numerical result $\tau(0) = 4.60 \cdot 10^{-23}$ s for an ultra-relativistic collision of oxygen and lead. This is slightly smaller than the value displayed in Fig. 1 ($4.74 \cdot 10^{-23}$ s) due to the average over the projectile disk.

The impact-parameter dependence of the transit time for a typical system according to (2.7) is displayed in the upper part of Figure 2. The time decreases smoothly from the central-collision value towards zero at the impact parameter corresponding to nuclear contact, $b = R + r$. Since the interaction time as well as the available center-of-mass energy attain large values only for central collisions, the investigation of processes such as plasma formation will focus on small impact parameters.

3. Available Energy and Maximum Energy Density

The center-of-mass energy $\sqrt{s(b)}$ for a collision at impact parameter b is determined from the laboratory energy per nucleon T/A_P and the mass numbers $N_P(b)$, $N_T(b)$ of the projectile and target participants, respectively, according to the standard Lorentz-invariant expression ($s = m_a^2 + m_b^2 + 2Tm_b$). The result is

$$\sqrt{s(b)} \tag{3.1}$$
$$= N_P(b) \cdot \text{amu} \cdot \left[1 + \left(\frac{N_T(b)}{N_P(b)}\right)^2 \left(1 + \frac{2N_P(b)\,T}{A_P N_T(b) \cdot \text{amu}}\right)\right]^{1/2},$$

where amu $= 0.9315$ GeV is the mass unit. The number of participants is obtained in the same geometrical model as the transit time (2.7). For the target participants I obtain

$$N_T(b) = \frac{3}{4} \frac{A_P^{2/3}}{r_0} \tau(b) \tag{3.2}$$

with $r = 1.2$ fm and $\tau(b)$ expressed in fermi. For central collisions, and without the averaging over the projectile disk, this can be approximated by the usual expression [1]

$$N_T(0) \simeq \tfrac{3}{2} A_P^{2/3} A_T^{1/3}, \tag{3.3}$$

which corresponds to the simple estimate obtained from a cylinder with length $2R$ and diameter $2r$ to simulate the overlap volume. It is equivalent to results obtained at lower energy in the fireball model. For impact parameters $b > R - r$, there is no complete overlap between projectile and target, and the number of participating projectile nucleons is given by

$$N_P(b) \simeq A_P \left[\frac{1}{2} + \frac{1}{2}\frac{R}{r} - \frac{1}{2}\frac{b}{r}\right]. \tag{3.4}$$

The impact-parameter dependence of the energy that is available in the interaction region calculated according to (3.1) for 200 GeV/nucleon $^{16}O + {}^{208}Pb$ is shown in the lower part of Figure 2. Neglecting the finite extension of the projectile, (3.1) can be approximated by

$$\sqrt{s(b)} \simeq A_p \cdot \text{amu} \cdot \left[1 + \frac{9(R^2 - b^2)}{4r_0^2 A_P^{2/3}} + \frac{3T(R^2 - b^2)^{1/2}}{r_0 A_P^{4/3} \cdot \text{amu}}\right]^{1/2}, \tag{3.5}$$

which becomes

$$\sqrt{s(b)} \;\rightarrow\; A_P^{1/3} \left[\frac{3}{r_0} T(R^2 - b^2)^{1/2} \cdot \text{amu}\right]^{1/2} \tag{3.6}$$

in the ultra-relativistic limit displayed by the dashed curve. It is evident that both available energy and transit time decrease rapidly with increasing impact parameter. Hence, nonequilibrium processes such as plasma formation will not occur with appreciable probability in peripheral collisions.

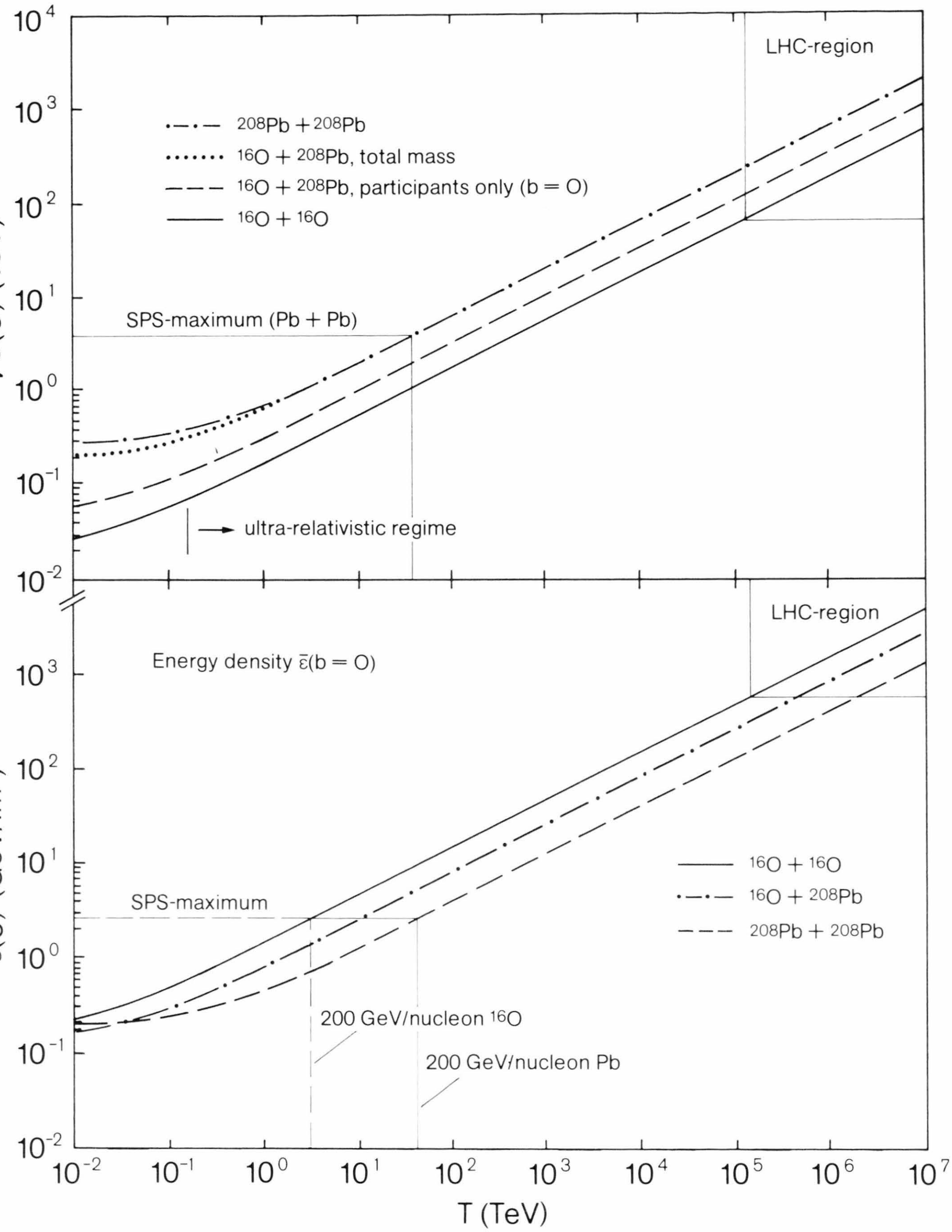

Fig. 3. Available center-of-mass energy for central collisions for three systems as a function of laboratory energy T (upper part). The system $^{16}O+Pb$ has been investigated at the SPS at $T=3.2$ TeV; the dotted curve displays the center-of-mass energy calculated with the total mass rather than the participants only. It is evident that the ultra-relativistic limit of the center-of-mass energy is reached at SPS-energies. The system Pb + Pb would result in a significant increase of the available energy. In the lower part, the maximum energy density attainable in central collisions is shown for the same systems as above.

For central collisions, the available center-of-mass energy is shown in the upper part of Fig. 3 for a number of systems as a function of laboratory energy T. In particular, the system $^{16}O+^{208}Pb$ serves as an example since it has been investigated at the SPS at 200 GeV/nucleon. Note that at this energy, the ultra-relativistic limit of the center-of-mass energy, $\sqrt{s(b)} = \sqrt{2N_T(b)\,T\,\mathrm{amu}}$, is attained as expected. For the system Pb + Pb, the maximum center-of-mass energy available in a central collision at 200 GeV/nucleon would be 4.02 TeV – still about a factor of 10 below the center-of-mass energy attainable at the planned relativistic heavy-ion-collider RHIC at Brookhaven with energies of about 0.1 TeV per nucleon in each beam, and far below the values obtainable with the proposed Large Hadron Collider (LHC).

Whereas the center-of-mass energy in the interaction region determines the upper limit of the energy that is available for nonequilibrium processes, it is the maximum energy density attainable in the collision that determines whether processes such as plasma formation may occur. (Whether they do occur is determined by the energy density actually attained, which depends on the interaction time.) Again I estimate the interaction volume $V(b)$ at impact parameter b in the simple geometrical approach used to obtain the transit time and the number of participants:

$$V(b) = \frac{\pi}{2} r \left\{ (b+r)\,[R^2-(b+r)^2]^{1/2} + R^2 \arcsin\frac{b+r}{R} + (r-b)\,[R^2-(b-r)^2]^{1/2} - R^2 \arcsin\frac{b-r}{R} \right\}. \quad (3.7)$$

In the limit $b=0$ this is approximated as

$$V(0) \simeq 2\pi\, r_0^3 A_P^{2/3} A_T^{1/3}. \quad (3.8)$$

This simple expression for the interaction volume corresponds to a cylinder with radius r and height $2R$ ($V(0) = 2\pi r^2 R$) as in the previous approximate expression (3.3) for the number of target participants. The volume of the Lorentz-contracted projectile is neglected at ultra-relativistic energies in the target rest frame. (Note that a larger value for the maximum energy density, and a somewhat different energy dependence would be obtained if the interaction volume were taken to be the Lorentz-contracted participant volume in the participant center-of-mass.)

With (3.1) and (3.8), an approximate expression (with the proper dependence on A_P, A_T) for the maximum energy density $\bar{\varepsilon}(0)$ attainable in the interaction region at $b=0$ is

$$\bar{\varepsilon}(0) \simeq \frac{\sqrt{s(0)}}{V(0)} \simeq \frac{A_P^{1/3}\cdot \mathrm{amu}}{2\pi\, r_0^3 A_T^{1/3}} \cdot \left[1+\left(\frac{3A_T^{1/3}}{2A_P^{1/3}}\right)^2 \left(1+\frac{4T}{3A_P^{2/3}\cdot A_T^{1/3}\cdot \mathrm{amu}}\right)\right]^{1/2}. \quad (3.9)$$

In the ultra-relativistic limit this becomes

$$\bar{\varepsilon}(0) \;\rightarrow\; \frac{[3A_P^{2/3}\cdot A_T^{1/3}\cdot T\cdot \mathrm{amu}]^{1/2}}{2\pi\, r_0^3 A_P^{2/3} A_T^{1/3}}. \quad (3.10)$$

Whereas this expression holds for asymmetric systems with $A_P \ll A_T$, the maximum energy density for symmetric systems $A_P \approx A_T = A$ is

$$\bar{\varepsilon}_s(0) \simeq \frac{3\sqrt{2}\,\mathrm{amu}}{4\pi\, r_0^3}\left[1+\frac{T}{A\,\mathrm{amu}}\right]^{1/2}, \quad (3.11)$$

which becomes

$$\bar{\varepsilon}_s(0) \;\rightarrow\; \frac{3[2T\,\mathrm{amu}]^{1/2}}{4\pi\, r_0^3 \sqrt{A}} \quad (3.12)$$

in the ultra-relativistic limit. At SPS-energies of 200 GeV/nucleon, these expressions yield $\bar{\varepsilon}(0) \simeq 1.41$ GeV/fm^3 for O + Pb and $\bar{\varepsilon}(0) \simeq 2.67$ GeV/fm^3 for Pb + Pb, or any other symmetric system such as O + O: In this simplified geometrical approach, the maximum energy density for symmetric systems at a given energy per nucleon is independent of the system size. However, it is obvious that larger systems provide both a larger ultra-relativistic limit of the transit time – and hence, of the interaction time – ($\tau = 2.02\cdot 10^{-23}$ s for oxygen, $4.74\cdot 10^{-23}$ s for lead) as well as an increase in the geometric cross section. Therefore, the probability of plasma formation as well as the probability to detect the corresponding physical signals is increased. This provides a motivation for the construction of heavy-ion injectors such as the Pb-injector at the SPS. Note, however, that SPS-energies may not yet suffice to generate the plasma due to the relatively low value of the maximum energy density.

The maximum energy density $\bar{\varepsilon}(0)$ calculated from (3.1) and (3.7) for $^{16}O+^{16}O$, $^{16}O+^{208}Pb$ and $^{208}Pb+^{208}Pb$ as function of laboratory energy is displayed in the lower part of Figure 3. At a given laboratory energy, the small O + O system exhibits the largest maximum energy density because of the small interaction volume; the approximate expression (3.12) may serve for a discussion of the A-dependence. (Note, however, that the energy density actually attained may have a different A-dependence.) The crossing point in $\bar{\varepsilon}(0)$ for asymmetric and symmetric systems with the same target mass number A_T that occurs at relatively low laboratory energies $T = T_c$ can be calculated in the geometrical approach

$$T_c \simeq \frac{2A_P^{2/3}\, A_T \,\text{amu}}{9\,A_P^{2/3} - 6\,A_T^{2/3}} \left[\frac{A_P^{2/3}}{A_T^{2/3}} - \frac{9}{4}\right], \qquad (3.13)$$

which yields $T_c \simeq 34$ GeV for $^{16}O + Pb$ and $Pb + Pb$, respectively. Beyond T_c, the asymmetric system provides a higher energy density at given laboratory energy T. In most cases, however, the laboratory energy per nucleon is the relevant quantity; at given T/A, $\bar{\varepsilon}(0)$ for the asymmetric system is below the value for the corresponding symmetric system as discussed before.

As in the calculation of the center-of-mass energy, it is obvious from Fig. 3 that at maximum SPS-energies the quantity $\bar{\varepsilon}(0)$ has safely reached the ultra-relativistic limit; it may, however, not yet be large enough to generate the plasma.

At LHC-energies (upper right corner in Fig. 3), on the other hand, the maximum energy density is certainly above the critical energy density for plasma formation predicted by lattice gauge theories (about 2.5 GeV/fm^3 [5]). Due to the constancy of the transit time τ^∞ in the ultra-relativistic limit, it is probable that a substantial fraction of this maximum energy density is actually attained and the plasma is formed – provided τ_{int} is sufficiently large.

In order to ensure such large values for the interaction time as well as for the geometric cross section, it is desirable to use systems of large mass numbers, rather than p+p or any other light system. In a collider experiment of $^{16}O + {}^{16}O$ at 64 TeV center-of-mass energy corresponding to $T = 137{,}449$ TeV, for example, we have $\bar{\varepsilon}(0) \simeq 553$ GeV/fm^3 according to (3.9) and $\tau \simeq 2.02 \cdot 10^{-23}$ s in a central collision. Hence, not only the maximum energy density but also the interaction time is sufficiently large to allow for plasma formation, whereas in a p+p collision at 4 TeV center-of-mass energy the short transit time may prevent plasma-generation in a non-equilibrium process, although the maximum energy density exceeds the critical value.

4. Conclusions

A straightforward macroscopic calculation of the transit times corresponding to nuclear contact and their impact-parameter dependence at relativistic energies has been performed. The transit time provides a lower limit of the interaction time. I have also estimated the maximum energy density attainable for various systems in this geometrical approach. This energy density is available for the formation of a quark-gluon plasma in a nonequilibrium process. Whether the plasma is formed depends on the actual energy density, which is a function of the interaction time. To ensure large values of the transit- and hence, interaction-time, it is obviously desirable to choose heavy systems such as Pb + Pb, rather than $^{16}O + Pb$. Due to the constancy of the transit time in the ultra-relativistic limit it is worthwhile to further enhance the center-of-mass energy in order to create the plasma. This provides a motivation for the design of a Large Hadron Collider suitable for very heavy ions.

I have not yet calculated the interaction time, which may be substantially larger than the transit time – for example, in case of full stopping. I have also not considered processes that occur in the condensation trail of deposited energy, in the region of space the fragments have passed through. They will effectively enhance the interaction time beyond the values obtained from nuclear contact: After the collision two pancakes (in the center-of-mass frame) recede at the speed of light, and quarks, gluons and hadrons contained in the region between them may create a local thermal equilibrium [6]. The energy that is deposited in the condensation region will essentially be converted into secondary hadrons. A calculation of the time scales involved in these processes will be of major interest.

[1] H. Satz, H. J. Specht, and R. Stock (eds.), Proc. 6th Int. Conf. on Ultra-Relativistic Nucleus-Nucleus-Collisions, in: Z. Physik **C 38,** Number 1/2 (1988).

[2] G. Wolschin, Nukleonika **22,** 1165 (1977); Fizika **9,** Suppl. 4, 513 (1977); Phys. Lett. **88 B,** 35 (1979); Nucl. Phys. **A 316,** 146 (1979); Proc. Int. School of Physics Varenna (R. A. Broglia, R. A. Ricci, and C. H. Dasso, eds.), North-Holland Publishing Co. 1981, p. 508.

[3] S. Ayik, G. Wolschin, and W. Nörenberg, Z. Physik **A 286,** 271 (1978). – R. Schmidt, V. D. Toneev, and G. Wolschin, Nucl. Phys. **A 311,** 247 (1978). – L. G. Moretto and G. J. Wozniak, Ann. Rev. Nucl. Part. Sci. **34,** 189 (1984).

[4] D. Strottman and A. S. Goldhaber, in: H. Satz, Nature London **324,** (13.11.1986) 116 (1986).

[5] T. Celik, J. Engels, and H. Satz, Nucl. Phys. **B 256,** 670 (1985).

[6] J. D. Bjorken, Phys. Rev. **D 27,** 140 (1983).